2021 43rd Annual International Conference of the
IEEE Engineering in Medicine & Biology Society (EMBC)
Oct 31 - Nov 4, 2021. Virtual Conference

A Wearable Walking Gait Speed-Sensing Device using Frequency Bifurcations of Multi-Resonator Inductive Link

Xinlei Yang, *IEEE Student Member*,
Le Jiang, Smith Giri, Sarah Ostadabbas, *IEEE Member*, and S. Abdollah Mirbozorgi, *IEEE Member*

***Abstract*— This paper describes a wearable inductive sensing system to monitor (i.e., sense and estimate) walking gait speed. This proposed design relies on the multi-resonance inductive link to quantify the angle of the human legs for calculating the speed of walking. The walking gait speed can be used to estimate the frailty in elderly patients with cancer. We have designed, optimized, and implemented a multi-resonator sensor unit to precisely measure the angle between human legs during walking. The couplings between resonators change by lateral displacements due to walking, and a reading coil senses the frequency bifurcations, corresponding to the changes in angle between legs. The proposed design is optimized using ANSYS HFSS and implemented using copper foil. The Specific Absorption Rate, SAR, in the human body is calculated 0.035 W/kg using the developed HFSS model. The operating frequency range of the proposed sensor is from 25 MHz to 46 MHz, and it can measure angles up to 90° (-45° to +45°). The measured resolution for estimating the angle shows the capability of the sensor for calculating the walking speed with a resolution of less than 0.1 m/s.**

***Keywords*—Walking Gait Speed, Wearable Sensor, Inductive Sensor, Frequency Bifurcation, ANSYS HFSS**

I. Introduction

Cancer is an age-related disease since ~60% of new cancer diagnoses and 70% of cancer-related deaths occur among adults aged 65 or more. Older adults with cancer are at high risk of treatment-related toxicity, and clinicians cannot assess the patient's performance status appropriately for evaluating the vulnerability [1]. It is required to personalize cancer treatment for older adults based on their frailty or anticipated tolerance of treatment. Prior studies have shown that a comprehensive multi-dimensional geriatric assessment can reliably predict cancer-related treatment failure. However, perceived complexity or concerns about the time and resources required for performing these assessments have led to their limited utilization [2].

The human activity data such as step count, gait speed, and total daily activity level can reveal the true functional age and reliably identify vulnerable older adults with cancer. Based on the American Society of Clinical Oncology, the walking gait speed is a reasonable assessment of function and physical performance (physical inactivity, loss of muscle mass, functional decline, etc.) in older adults with cancer [3].

There is no reliable approach for oncologists to collect satisfactory data on the physical activity or frailty of older adults with cancer. Either they must perform a physical test in their office to determine the gait speed of each patient, or they must rely on the memory of their patients, which can be unreliable [4], [5].

There are different types of camera tracking systems for gait speed monitoring. The camera-based gait speed detection approaches need a fixed setup of multiple cameras and a synchronization/processing station, limiting their access to only specific areas. Camera-based approaches rely on a one-time measurement in the clinic and do not reflect typical day-to-day activities of patients during a day or a week [6]. Moreover, any video-based monitoring system is hindered by privacy issues.

Using a multimodal non-vision sensor array could be the solution to overcome these barriers; nonetheless, sensor technologies for indoor precise displacement monitoring are still in their developmental stage. For example, measuring foot pressure cannot provide an estimate of the distance taken [7]. Available devices that patients can take home to record concrete numbers on their activity are pedometers and other fitness trackers such as Fitbit and Apple Watches. These devices cannot detect the distance taken (only collect data on the steps taken) and are inaccurate for calculating the walking gait speed [8]-[12]. For example, the smartphone base sensor and software can only be used to count steps and average walking speed (with a predefined distance) and cannot calculate/monitor real-time data [12].

None of the aforementioned technologies is accurate and convenient enough to be considered a standalone wearable device for 24/7 monitoring of patient's gait speed and their other daily physical activities. We have designed and implemented a novel sensor unit to measure the angle between human legs to estimate the walking gait speed based on coupling variations of coupled inductors. The coupling variations can be detected by measuring the changes of resonance frequency bifurcations [13]. The principle and conceptual schematic are shown in Figure 1a. We describe the

Xinlei Yang is a graduate student at the Electrical and Computing Engineering Department, University of Alabama at Birmingham, Birmingham, AL 35294 USA (email: y1995815@uab.edu)

Smith Giri is with the Department of Medicine, Division of Hematology/Oncology, the University of Alabama at Birmingham, Birmingham, AL 35233 USA (email: smithgiri@uabmc.edu)

Le Jiang and Sarah Ostadabbas are with the Electrical and Computing Engineering Department, Northeastern University, Boston, MA 02115 USA (emails: jiang.l@northeastern.edu, ostadabbas@ece.neu.edu)

S. Abdollah Mirbozorgi: Electrical and Computing Engineering Department, the University of Alabama at Birmingham, Birmingham, AL 35294 USA (phone: 205-934-8412; email: samir@uab.edu)

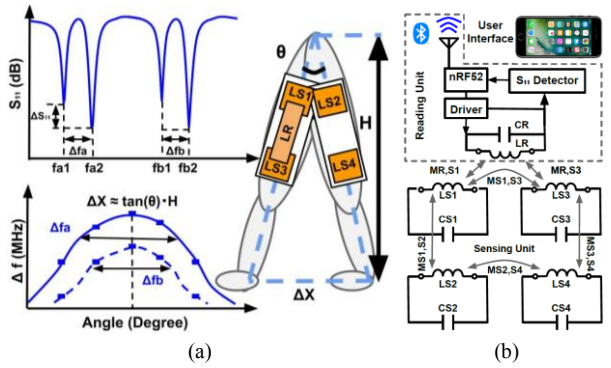

(a) (b)

Figure 1. (a) The principle and conceptual schematic of the proposed design indicating the locations of the sensors, multiple bifurcations, and the mechanism of the body displacement calculation. (b) The hardware block diagram and equivalent circuit model of the proposed design.

design process and present the ANSYS HFSS simulation results in Section II. Then, we present the measurement results in Section III, followed by a conclusion in Section IV.

II. Design Review and Process

A. Design Review

The conceptual schematic and working principle of the proposed gait speeding monitoring system are shown in Figure 1a. To measure the distance taken and calculate the gait speed, we propose to measure the angle between legs during walking. To estimate the angle between the human legs, we propose to locate four resonators between the legs, above the knees, and configure two coupled-resonator pairs. These resonators are tuned to generate 4 resonance frequencies. Any changes in the coupling between the resonator pairs shift the resonance frequencies and change the frequency bifurcations level [13], [14]. The human legs during walking swing like a pendulum, while the resonators are attached to the legs. Therefore, it causes a large lateral misalignment between the resonators and significant changes in couplings. Since the coupling changes between each pair of the resonators affect the resonances equally, while the shifts in the resonance frequencies occur in opposite directions, this method provides the capability of measuring the changes of the target parameter (angle) differentially. Therefore, the angle between the legs corresponds to the Δf (differential changes in the resonance), which makes the sensing more reliable and less sensitive to the noise of measurement circuitries and coils' unwanted environmental variations. So, the angle calculation is based on the relative displacement of the resonators and Δf, not the absolute value of a shift in a single resonance. Two pairs of resonators are used to improve angle detection sensitivity, covering large angles up to 90°. Figure 1a shows the locations of the sensors (resonators) and their multiple frequency bifurcations, too.

Figure 1b illustrates the hardware circuit block diagram and the inductive link equivalent circuit of the sensing unit. The proposed design consists of four sensing resonators (LS1-LS4), a reading coil (LR), a circuit interface (driver and S_{11} detector), and a processing unit (nRF52 module). The processor is equipped with a Bluetooth transceiver to exchange data with a smartphone.

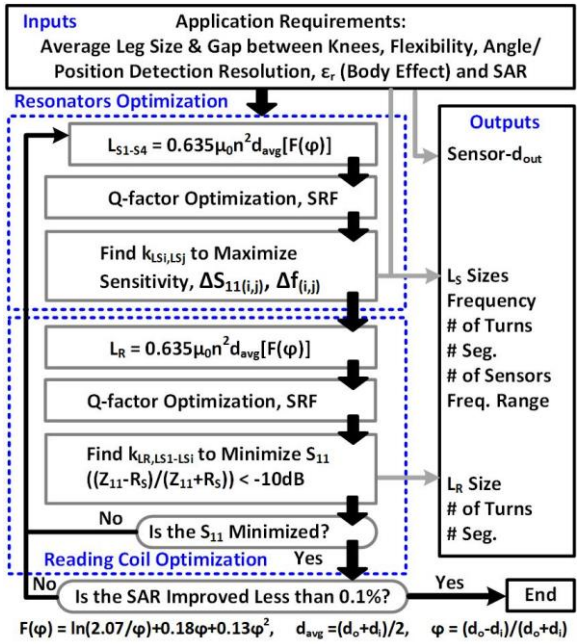

Figure 2. The flowchart of design and optimization process for the proposed inductive link.

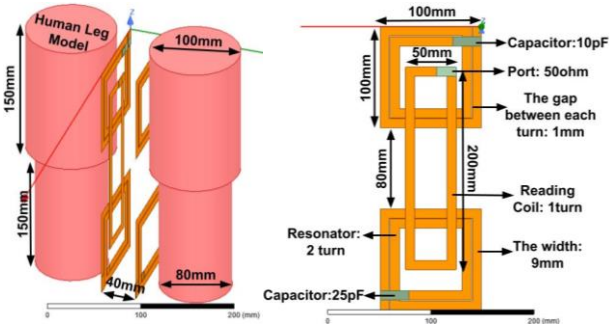

(a) (b)

Figure 3. (a) The HFSS model of the proposed inductive sensor and human body model, and (b) the optimized inductive sensor (reading coil and two of resonators), indicating the dimensions.

Figure 2 shows the flowchart of the design flow and optimization of the sensing inductive link for the resonators and the reading coil. The Inputs box includes the application requirements and parameters to be considered for the design, and the Outputs box lists the obtained parameters of the design after optimization. Using the optimization process of Figure 2, we have determined the size, the number of the turns, working frequencies, and gaps between the resonators and reading coil for all inductors in the proposed design. Theoretical modeling and HFSS simulations of the inductors are performed for the optimization.

B. Simulation Results

We have modeled the proposed sensing wearable, including the inductive link (two pairs of resonators and reading coil) and human legs, using HFSS software to support the design and optimization process. Based on the outcomes of the design process presented in Figure 2 and the developed HFSS model, the optimum outer diameters of the resonators and the reading coil have been determined to be 10 cm × 10

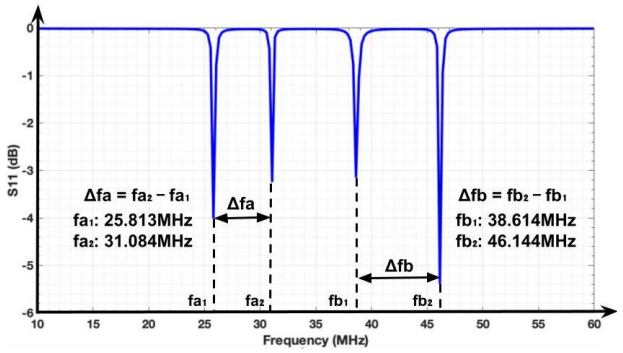

Figure 4. The HFSS simulation results, S_{11} as a function of frequency at 0° angle between legs model.

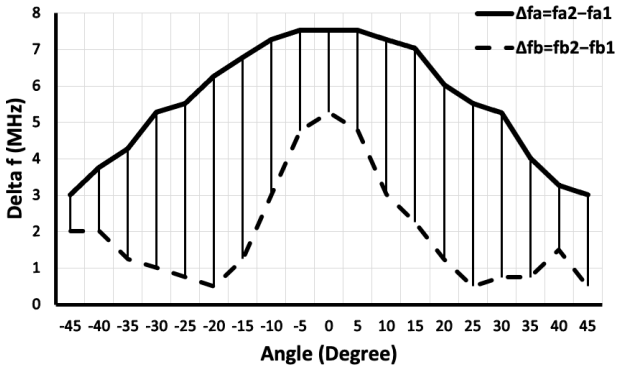

Figure 5. The HFSS results, indicating Δf vs angle between legs.

cm and 6 cm × 24 cm, respectively. The gap between the resonators equals 8 cm for both resonator pairs on the left and right legs. The developed HFSS model of the proposed sensing system is presented in Figure 3a, and the details of the coils' dimensions are provided in Figure 3b. The best performance on sensing (highest qualities of the resonances on reflection coefficient S_{11}) is obtained for the frequency range of 25 MHz to 46 MHz. The optimization target was to maximize the shifts and changes in the quality of the resonance frequencies due to changes of the couplings for achieving the maximum possible sensitivity. The capacitors of the resonators are selected based on the frequency range, 25 pF for L_1 and L_2, and 50 pF for L_3 and L_4. The HFSS simulation results are presented in Figure 4 (S_{11} as a function of frequency), indicating four resonances (two sets of frequency bifurcations), in which each of the upper and lower resonator pairs generates one frequency bifurcation (made of two resonances).

In our HFSS model, we have rotated one of the legs (and associated resonators) to create an angle between the legs. This misalignment between the resonators has changed the mutual couplings between them and caused significant shifts in the resonance frequencies. This process is repeated for different angles, and calculated shifts of frequency (Δf) are presented in Figure 5 for both upper (L_1 and L_2) and lower (L_3 and L_4) resonator pairs. These results show the capability of the sensing system for accurately monitoring the angles between legs from -45° to +45°. The upper resonator pair provides significant Δf changes as a function of angle for angles bigger than |±20°|, and the lower resonator pair provides linear Δf changes for the angles less than |±20°|.

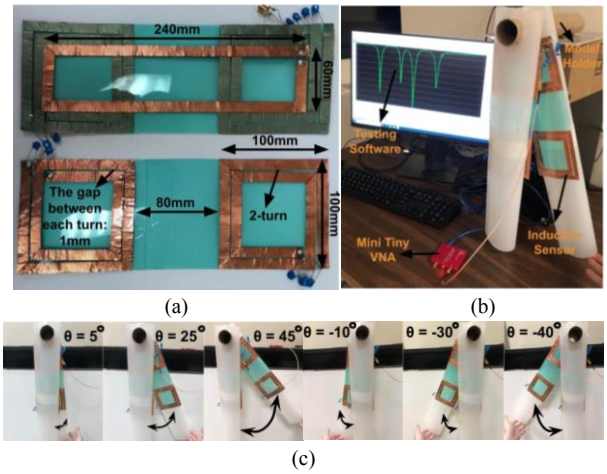

Figure 6. (a) The implemented prototype the proposed sensor unit, including the resonators and reading coil, and (b) the test setup used to characterize the performance of the design. (c) The approach of testing the system from different angles (5°, 25°, 45°, -10°, -30°, -40°).

The HFSS model is also used to evaluate the Specific Absorption Rate, SAR, in the human body regarding safety concerns. The average SAR is calculated 0.035 W/kg at the highest resonance frequency, worst-case scenario, while the input power was set 100 mW (required for proper detection of the coupling between the resonators). Therefore, the SAR level would be 45 times smaller than the standard limits of the 1.6 W/kg.

III. Measurement Results

The inductive sensing unit is implemented using 9 mm copper foil with a 0.1 mm thickness, including four resonators and a reading coil. The schematic of the implemented prototype is shown in Figure 6a, indicating the measured dimensions. A Vector Network Analyzer, VNA, is connected to the reading coil through an SMA connector to measure its reflection coefficient, S_{11}. Figure 6b shows the test setup, including the implemented prototype and its arrangement on the legs plastic model, VNA, and a computer to display the results. This setup is prepared for measuring S_{11} and evaluating the level of the multiple resonance frequency bifurcations and shifts with changing the location of the resonators within legs. The reading coil is made of one turn of the copper foil with outer dimensions of 6 cm ×24 cm, while the resonators are made of two turns of the copper foil with outer dimensions of 10 cm ×10 cm. To tune the resonance frequencies within the desired range (25 MHz - 46 MHz), 25 pF and 50 pF capacitors are utilized for the upper and lower resonator pairs, respectively.

Figure 6c shows the approach used to test the system by creating the different angles (5°, 25°, 45°, -10°, -30°, -40°) between the legs model. The measured S_{11}s are presented in Figure 7, including the results of 0° and 40° with significant shifts in the resonance frequencies. The angle between the legs model is changed from -45° to +45° with 5°steps, and the Δfs are measured. Figure 8 presents the measured Δf as a function of angle for both the upper and lower resonator pairs. The results obtained from the upper resonator pair will be used to estimate large angles, and the results of the lower

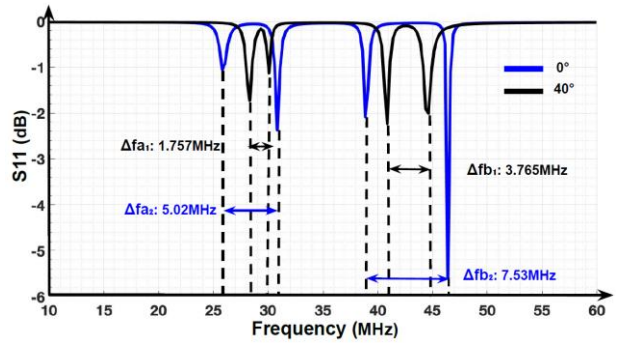

Figure 7. The measured S_{11} results at different angles (0° and 40°).

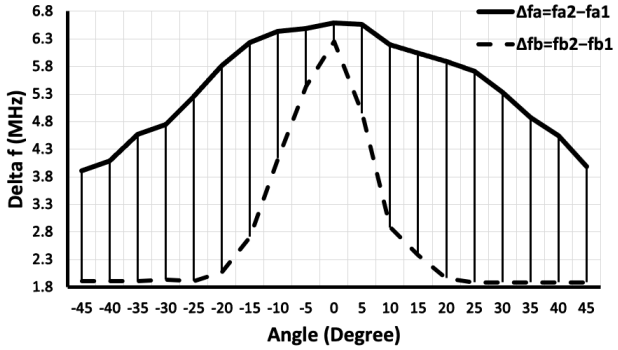

Figure 8. The experimental results of the Δf as a function of the angle between the legs model of Figure 6b.

resonator pair will be used for estimating the small angles accurately. The measured results of Figure 8 can be summarized in an equation/correlation to show the relationship between θ and Δf.

$$\theta = \begin{cases} 0.0758 \cdot \Delta fa + 7.1944 & -45° \le \theta \le -20° \\ 0.222 \cdot \Delta fb + 6.3406 & -20° \le \theta \le 0° \\ -0.2231 \cdot \Delta fb + 5.9172 & 0° \le \theta \le +20° \\ -0.0786 \cdot \Delta fa + 7.586 & +20 \le \theta \le +45° \end{cases} \quad (1)$$

The displacement or distance taken by each step (Δx) can be obtained considering the waist height (H) and (2).

$$\Delta x = H \cdot \tan(\theta) \quad (2)$$

The period of each step will be measured using the processor of the system for calculating the walking gait speed (Gait Speed = $\frac{\Delta x}{t}$).

We have calculated the gait speed resolution of this device based on the measured results. By assuming of 1 s for the period of each step, 1° of sensitivity in measuring θ, and H = 75 cm, the resolutions for angles from -20° to 20° and angles from ±20° to ±45° are 0.98 cm/s and 1.25 cm/s, respectively. To detect 1° of changes using the proposed sensing unit, the circuit interface must have the capability of measuring S_{11} changes with the resolution of < 200 kHz and < 80 kHz in Δf for angles from -20° to 20° and angles from ±20° to ±45°, respectively.

The calibration of the proposed design regarding the variation of the gap between legs for different users will be part of our future work. The calibration process will be performed by collecting data from multiple experiments and use it to develop a machine learning algorithm and train it to apply the required correction to the measured data adaptively and provides robust estimating of the walking gait speed.

IV. Conclusion

We have developed a wearable walking gait speed sensing device based on the frequency bifurcation phenomenon of coupled inductive resonators. The proposed design relies on calculating the angle between human legs to estimate the distance has taken and gait speed. We have modeled the sensing unit and human legs in ANSYS HFSS to optimize the design. We have implemented a prototype to verify the functionality of the proposed sensing unit and characterize its performance. The implemented prototype includes a reading coil and four resonators, made of copper foil, to measure the angle between legs accurately. The experimental results have confirmed that the sensing unit can accurately measure the angle changes from -45° to +45°, with the operating frequency from 25 MHz to 46 MHz. The measured angle results by the prototype show the capability of the proposed design in sensing the walking gait speed with a resolution of less than 0.1 m/s.

References

[1] E. Celis, D. Li, Y. Yuan, Y.M. Lau, A. Hurria, "Functional versus chronological age: geriatric assessments to guide decision making in older patients with cancer," *Lancet Oncol.*, vol. 19, no. 6, pp. 305-316. Jun. 2018.

[2] S.G. Mohile, et al., "Practical Assessment and Management of Vulnerabilities in Older Patients Receiving Chemotherapy: ASCO Guideline for Geriatric Oncology," *Journal of Clinical Oncology*, vol. 36, no. 22, pp. 2326-2347, 2018.

[3] M.E. Hamaker, M.C. Prins, R. Stauder, "The relevance of a geriatric assessment for elderly patients with a hematological malignancy a systematic review," *Leukemia Res.,* vol. 38 no. 3, pp. 275-283, 2014.

[4] L.V. Ojeda, J. Rebula, A.D. Kuo, P.G. Adamczyk, "Influence of contextual task constraints on preferred stride parameters and their variabilities during human walking," *Med. Eng. Phys.,* vol. 37, no. 10, pp. 929–936, 2015.

[5] M. Herran, B.G. Zapirain, and A.M. Zorrilla, "Gait Analysis Methods: An Overview of Wearable and Non-Wearable Systems, Highlighting Clinical Applications," *Sensors,* vol. 14, no. 2, pp. 3362–3394, 2014.

[6] B. Muñoz, et al., "Automated Gait Analysis using a Kinect Camera and Wavelets," *IEEE International Conference on e-Health Networking, Applications and Services (Healthcom),* pp. 1-5, Ostrava, 2018.

[7] K. Kong and M. Tomizuka, "A Gait Monitoring System Based on Air Pressure Sensors Embedded in a Shoe," *IEEE/ASME Transactions on Mechatronics,* vol. 14, no. 3, pp. 358-370, Jun. 2009.

[8] W. Wang and P.G. Adamczyk, "Analyzing Gait in the Real World Using Wearable Movement Sensors and Frequently Repeated Movement Paths," *Sensors (Basel),* vol. 19, no. 8, Apr. 2019.

[9] R. McGinnis, et al., "A Machine Learning Approach For Gait Speed Estimation Using Skin-mounted Wearable Sensors: From Healthy Controls to Individuals with Multiple Sclerosis," *PLOS ONE,* vol. 12, no. 6, Jun. 2017.

[10] R. Hanton, et al., "Mobile Phone-based Measures of Activity, Step Count, and Gait Speed: Results from a Study of Older Ambulatory Adults in a Naturalistic Setting," *JMIR Mhealth Uhealth,* vol. 5, no. 10, Oct. 2017.

[11] J. Martin, et al., "Pedometer Accuracy in Slow Walking Older Adults," *Int J Ther Rehabil,* vol. 19, no. 7, pp. 387-393, Jul. 2012.

[12] C. Hurt, et al., "Assessing a Novel Way to Measure Step Count While Walking Using a Custom Mobile Phone Application," *PLOS ONE,* vol. 13, no. 11, Nov. 2018.

[13] J.I. Sancho, N. Perez, J. DeNó, J. Mendizabal, "Implementation of Simultaneous Multi-Parameter Monitoring Based in LC-Type Passive Wireless Sensing with Partial Overlapping and Decoupling Coils," *Sensors (Basel),* vol. 19, no. 23, 2019.

[14] Q. Tan, T. Luo, T. Wei, J. Liu, L. Lin, J. Xiong, "A Wireless Passive Pressure and Temperature Sensor via a Dual LC Resonant Circuit in Harsh Environments," *Journal of Microelectromechanical Systems,* vol. 26, no. 2, pp. 351-356, Apr. 2017.